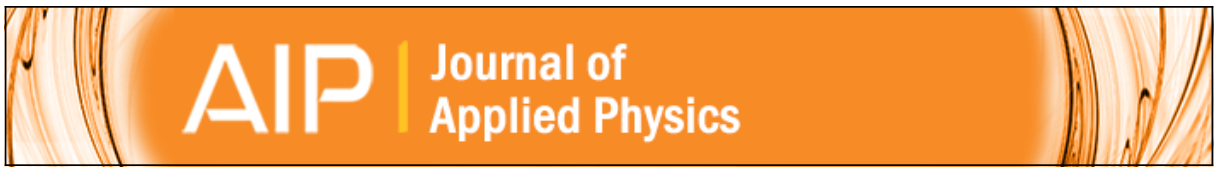

Ab initio studies on the mechanism for linear and nonlinear optical effects in YAl3(BO3)4

Ran He, Z. S. Lin, M.-H. Lee, and C. T. Chen

Citation: Journal of Applied Physics **109**, 103510 (2011); doi: 10.1063/1.3587571

View online: http://dx.doi.org/10.1063/1.3587571

View Table of Contents: http://scitation.aip.org/content/aip/journal/jap/109/10?ver=pdfcov

Published by the AIP Publishing

Ab initio studies on the mechanism for linear and nonlinear optical effects in $YAl_3(BO_3)_4$

Ran He,[1,3] Z. S. Lin,[1,a)] M.-H. Lee,[2] and C. T. Chen[1]
[1]*Beijing Center for Crystal R&D, Key Laboratory of Functional Crystals and Laser Technology, Technical Institute of Physics and Chemistry, Chinese Academy of Sciences, P.O. Box 2711, Beijing 100190, China*
[2]*Department of Physics, Tamkang University, Tamsui, Taipei 25137, Taiwan*
[3]*Graduate University of Chinese Academy of Sciences, Beijing 100049, P.R. China*

(Received 24 February 2011; accepted 31 March 2011; published online 17 May 2011)

First-principles studies of the linear and nonlinear optical properties for $YAl_3(BO_3)_4$ (YAB) are presented. Based upon the electronic band structure, the optical refractive indices, birefringence, and second harmonic generation (SHG) coefficients of YAB are calculated, which are in good agreement with experimental values. In addition, the SHG-weighted electron density analysis and the real-space atom-cutting method are adopted to elucidate the origin of the linear and nonlinear optical effects in YAB. The results show that the anionic (BO_3) groups have dominant contributions to the birefringence. The contribution of the Al cations to the optical effects is negligibly small. However, the Y cations bond to the neighbor O anions and form the deformed (YO_6) octahedra, which results in the large SHG effects in YAB. © *2011 American Institute of Physics*. [doi:10.1063/1.3587571]

I. INTRODUCTION

Discovered in the 1960s,[1] $YAl_3(BO_3)_4$ (YAB) belongs to the family of $A_xM_{1-x}Z_3(BO_3)_4$ (A, M = Y, La, and rare earths; Z = Al, Ga, and Sc), which are known as the self-frequency doublers. As early as 1974, the YAB crystal was reported as a very effective second-harmonic (SHG) generation material.[2] This crystal possesses a wide transmission range from the deep ultraviolet (UV) to the infrared spectrum regions (165–2200 nm), a moderate anisotropy of the refractive index ($\Delta n = 0.0684$ at 1064 nm), large nonlinear coefficients ($d_{11} = 1.7$ pm/V), a short SHG wavelength ($\lambda^{SHG}_{shortest} \sim 210$ nm), relatively high hardness (Mohs 7.5), and good chemical stability.[3] Recently, the YAB single crystals with high optical quality have been obtained with the dimension of $16 \times 16 \times 18$ mm.[4] Therefore, YAB is a very promising nonlinear optical (NLO) crystal for the fourth harmonic generation (266 nm) of the Nd:YAG lasers.

The YAB crystal has a trigonal structure with the space group of $R32$, and its primitive cell is shown in Fig. 1. Traditionally, one may categorize the basic structure units of YAB as Al^{3+} and Y^{3+} cations and $(BO_3)^{3-}$ anionic groups. Both Al^{3+} and Y^{3+} cations are six-coordinated to the neighbor O atoms, while each $(BO_3)^{3-}$ anionic group is in a planar trigonal shape and perpendicular to the optical z-axis. It is well known that the $(BO_3)^{3-}$ anionic groups are the microscopic units which dominantly contribute to the SHG effects in the KBBF-type UV borate NLO crystals, including $KBe_2BO_3F_2$ (KBBF),[5] $K_2Al_2B_2O_7$ (KABO), $BaAl_2B_2O_7$ (BABO),[6] and $BaAlBO_3F$ (BABF).[7] The comparison among their SHG coefficients shows, however, that YAB has a much larger SHG coefficient (see Table I). The SHG coefficient of YAB is even slightly larger than that of the borate NLO crystal β-BaB_2O_4 ($d_{22} = 1.60$ pm/V),[8,9] in which the planar (B_3O_6) microscopic unit is expected to produce much larger microscopic second-order susceptibilities than the $(BO_3)^{3-}$ anionic group. Therefore, it is highly desirable to understand the mechanism of why the YAB crystal has extremely large NLO effects. This can effectively prompt the development of new UV NLO crystals via the molecular engineering approach.

In 2007, Wang *et al*. calculated the linear optical properties of YAB by the density functional theory,[10] and their results were in reasonable agreement with the experimental values.[3] However, to our best knowledge, there has been a lack of *ab initio* studies on its NLO effects. In this work, we investigate the electronic structures, and linear and nonlinear optical properties in YAB using the plane-wave pseudopotential method. Combined with the SHG-weighted electron density analysis and the real-space atom-cutting technique, we find that the virtual transition processes between the Y cations and the neighbor O anions have much larger contributions to the SHG effects compared to the $(BO_3)^{3-}$ anionic groups, although the latter microscopic units have the dominant contribution to the birefringence in YAB.

II. METHODS AND COMPUTATIONAL DETAILS

The plane-wave pseudopotential method is employed to solve the electronic structure of YAB with the local density function approximation (LDA).[11] Ultrasoft pseudopotentials allow us to use a small plane wave basis set with a kinetic-energy cutoff of 500 eV without sacrificing accuracy. K-point meshes with a density of $(5 \times 5 \times 5)$ points in the Brillouin zone of the YAB primitive cell are adopted. We have determined that the choice of these computational parameters is sufficient to ensure a good convergence for the current studies.

It is well known that the bandgap calculated by the LDA is usually smaller than the experimental data due to the

a)Author to whom correspondence should be addressed. Electronic mail: zslin@mail.ipc.ac.cn.

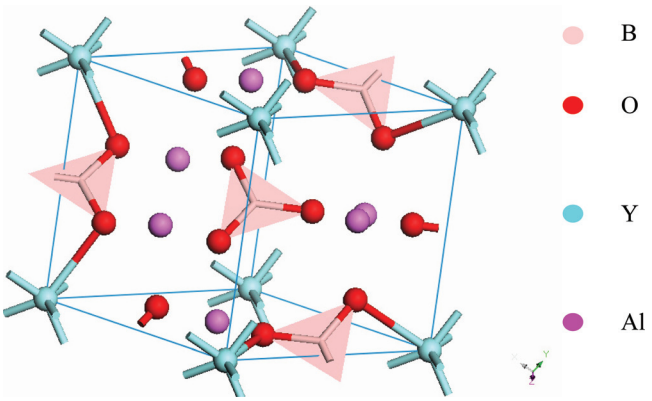

FIG. 1. (Color online) Primitive cell of YAB.

discontinuity of exchange-correlation energy. A scissors operator is therefore used to shift upward all of the conduction bands to agree with the experimental bandgap.

Based on the electronic band structure, the refractive indices are obtained from the real part of the dielectric constants, which can be obtained from its imaginary part using the Kramers–Kronig transformation. The imaginary part can be calculated with the momentum matrix elements between occupied and unoccupied electronic states.[12] Moreover, the SHG coefficients are calculate according to,[9,13]

$$\chi^{\alpha\beta\gamma} = \chi^{\alpha\beta\gamma}(VE) + \chi^{\alpha\beta\gamma}(VH) + \chi^{\alpha\beta\gamma}(\text{two bands}), \quad (1)$$

$$\chi^{\alpha\beta\gamma}(VH) = \frac{e^3}{2\hbar^2 m^3}\sum_{vv'c}\int\frac{d^3k}{4\pi^3}p(\alpha\beta\gamma)\mathrm{Im}[p^{\alpha}_{vv'}p^{\beta}_{v'c}p^{\gamma}_{cv}] \times\left(\frac{1}{\omega^3_{cv}\omega^2_{v'c}}+\frac{2}{\omega^4_{vc}\omega_{cv'}}\right), \quad (2)$$

$$\chi^{\alpha\beta\gamma}(VE) = \frac{e^3}{2\hbar^2 m^3}\sum_{vcc'}\int\frac{d^3k}{4\pi^3}p(\alpha\beta\gamma)\mathrm{Im}[p^{\alpha}_{vc}p^{\beta}_{cc'}p^{\gamma}_{c'v}] \times\left(\frac{1}{\omega^3_{cv}\omega^2_{vc'}}+\frac{2}{\omega^4_{vc}\omega_{c'v}}\right), \quad (3)$$

$$\chi^{\alpha\beta\gamma}(\text{two bands}) = \frac{e^3}{\hbar^2 m^3}\sum_{vc}\int\frac{d^3k}{4\pi^3}p(\alpha\beta\gamma)\mathrm{Im}[p^{\alpha}_{vc}p^{\beta}_{cv}(p^{\gamma}_{vv}-p^{\gamma}_{cc})], \quad (4)$$

TABLE I. Comparison of birefringence (Δn) and SHG coefficients (d_{ij}) of KBBF, KABO, BABO, BABF, and YAB at the wavelength of 1064 nm.

	Δn	d_{11} (pm/V)
KBBF[a]	0.080	0.47
KABO[b]	0.068	0.48
BABO[c]	0.053	0.745
BABF[d]	0.042	0.702
YAB[e]	0.068	1.70

[a]Reference 21.
[b]Reference 22.
[c]Reference 23.
[d]Reference 24.
[e]Reference 3.

where α, β, and γ are Cartesian components, v and v' denote valence bands, and c and c' denote conduction bands; $p(\alpha\beta\gamma)$ denotes full permutation and explicitly shows the Kleinman symmetry of the SHG coefficients. The band energy difference and momentum matrix elements between the ith and jth states are denoted as $\hbar\omega_{ij}$ and p^{α}_{ij}, respectively, and they are all implicitly k dependent. $\chi^{\alpha\beta\gamma}(VE)$ and $\chi^{\alpha\beta\gamma}(VH)$ give the contributions to χ^2 from virtual-electron (VE) processes and virtual-hole (VH) processes, respectively, and $\chi^{\alpha\beta\gamma}$(two bands) is the contribution to χ^2 from the two-bands processes, which is negligibly small in most NLO oxide crystals.

In order to identify the orbitals or bands contributing the SHG most in a molecule or a solid, a SHG-weighted electron density analysis is devised.[14,15] In this scheme, the considered SHG coefficient is "resolved" onto each orbital or band, and then the SHG-weighted bands are used to sum the probability densities of all occupied (valence) or unoccupied (conduction) states. This ensures that the quantum states irrelevant to SHG are not shown in the occupied or unoccupied "SHG-densities," while the orbitals vital to SHG are intuitively highlighted in the real space. Moreover, to investigate the influence of the ions on the crystal's optical response, a real-space atom-cutting method is also used. The contribution of ion A to the nth order susceptibility denoted as $\chi^{(n)}(A)$, and evaluated according to Ref. 10,

$$\chi^{(n)}(A) = \chi^{(n)}(\text{all ions except } A \text{ are cut}), \quad (5)$$

i.e., it can be obtained by cutting all ions except A from the original wave functions.

III. RESULTS AND DISCUSSION

The calculated band structures of YAB along the lines of symmetry are shown in Fig. 2. YAB has a direct bandgap of 5.57 eV at the G point, which is less than the experimental value of 7.5 eV (~165 nm).[4] Figure 3 displays the density of states (DOS) and partial (PDOS) of the respective species in YAB. Clearly, the energy bands can be divided into several regions. The very low region of the valence bands (VB) are composed of Y 4*s* orbitals, which are strongly localized at

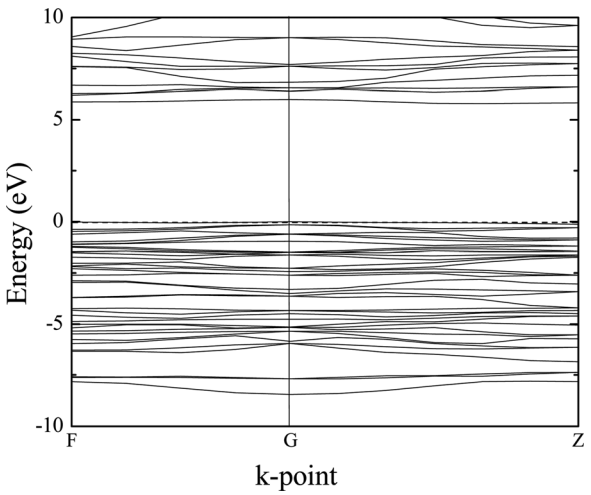

FIG. 2. Band structure of YAB.

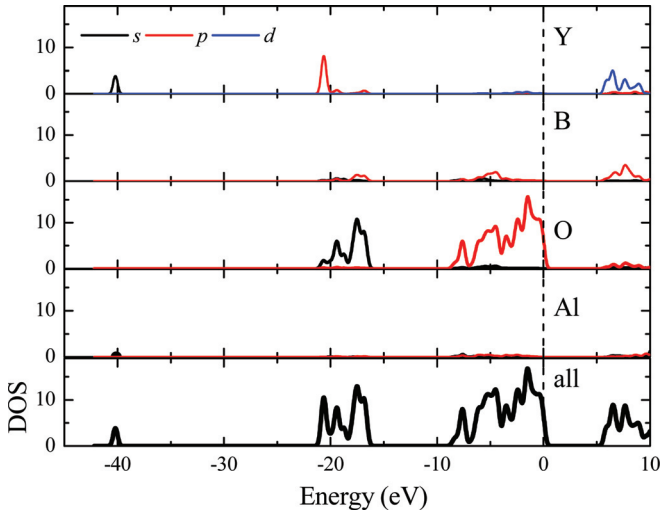

FIG. 3. (Color online) DOS and PDOS plots of YAB.

about −40 eV. The middle region of VB from −21 to −14 eV are mainly composed of Y 4*p* and O 2*s* orbitals. The upper one (from −8 to 0 eV) are composed of O 2*p*, and B 2*s* and 2*p* orbitals, but the very top of the VB is dominant by O 2*p* orbitals. The bottom of the conductive bands (CB) is mainly composed of Y 4*d* and B 2*p* orbitals, and the Y 4*d* orbitals determine the CB minimum of YAB. The orbitals on Al, on the contrary, have very little contribution to the overall electronic structures. All of these electronic characteristics are consistent with those obtained by Wang *et al.*[10]

The calculated refractive indices as a function of different frequencies are shown in Fig. 4, which are in good agreement with the experimental value. Meanwhile, the calculated SHG coefficient of YAB is $d_{11} = 1.65$ pm/V, which is also very close to the experimental value (1.7 pm/V). These agreements prove the validity of our studies on YAB with the LDA plane-wave pseudopotential method. Alternatively, it is known that the LDA method usually yields an incorrect electronic structure for the materials which include the elements that contain *d* or *f* orbitals. This is because there is no exactly solution to parameterize the generalized exchange-correlation energy. So in this work the LDA + U method[16,17] is also adopted by explicitly adding an additional orbital-dependent interaction, Hubbard U, to the LDA Hamiltonian. We found that actually the choice of U (from 0.0 to 8.0 eV) does not affect the relative position of the Y 4*d* orbitals, which are always located at the CB minimum. Consequently, the optical properties in YAB are almost independent of the Hubbard energy, U.

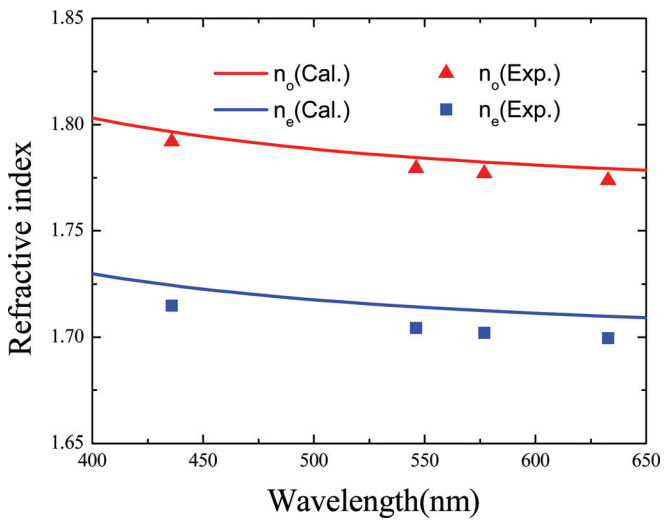

FIG. 4. (Color online) Comparison of the calculated and experimental refractive index dispersion of YAB (experimental values from Ref. 25).

Figure 5 plots the SHG-weighted electron densities of the occupied and unoccupied orbitals on the planes containing the (BO_3) groups and Y-Al ions, respectively. Here we only consider the VE processes since they have dominant contributions to the SHG effects (>70%) in YAB. It is clear that both occupied and unoccupied states of the Al cations, in analogy to the alkali metal or alkali earth metal ions in the KBBF-type NLO crystals,[18] have almost no effect on the SHG, indicating their strong ionic characteristics. The occupied states contributed to SHG mainly come from the O 2*p* orbitals, while the unoccupied states mainly come from the Y 4*d* orbitals. The conduction bands of the B 2*p* orbitals also have some contributions. This means that the VE processes from the O valence states to the Y and B conduction states determine the SHG effects in YAB. Therefore, apart form the $(BO_3)^{3-}$ anionic group, the $(YO_6)^{9-}$ anionic group formed by the Y^{3+} cation and the neighbor O^{2-} anions must be considered as the NLO active microscopic unit. Namely, the isolated Y^{3+} cation does not contribute to SHG effects in YAB alone. In fact, the Y-O bond lengths (2.30 Å) in the (YO_6) octahedron are in the range of those in the yttrium oxide (2.24–2.33 Å).

To investigate the influence of the respective ions and groups on the linear and nonlinear optical response of YAB,

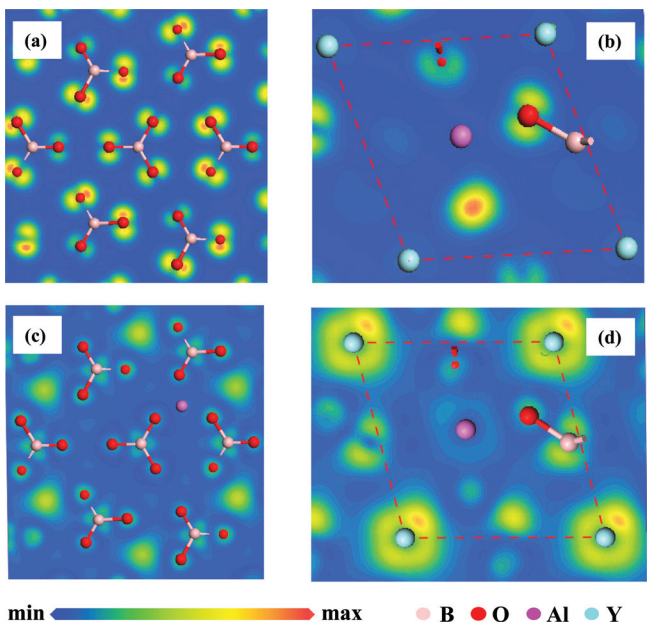

FIG. 5. (Color online) SHG-weighted electron densities of the occupied (valence) orbitals in (a) the (BO_3) plane, (b) the Y-Al plane, and those of the unoccupied (conduction) orbitals in (c) the (BO_3) plane and (d) the Y-Al plane in the VE processes.

we employ the real-space atom-cutting method. According to the previously discussed SHG-weighted electron density analysis, the NLO microscopic units are categorized as follows; the Al^{3+} cations, the $(BO_3)^{3-}$ anionic groups, and the $(YO_6)^{9-}$ anionic groups. Our previous studies showed that the electron density around the cations which exhibit strong ionic characteristics is spherical,[18] so we choose the cutting radius of Al to be 0.55 Å. Following the rule of keeping the cutting spheres of Al and O in contact, the cutting radius of O is set to be 1.30 Å. For the boron and yttrium atoms, the cutting radii are chosen as 0.70 and 1.20 Å, respectively. Our test showed that, in fact, the atom-cutting analysis results are insensitive to the choices of the cutting radii in YAB.

The atom-cutting analysis results of the linear and nonlinear optical properties in YAB are listed in Table II. Several interesting conclusions can be deduced. (i) The contribution of the Al^{3+} cation to both linear and nonlinear optical effects of YAB is negligibly small. This also confirms the SHG-weighted electron density analysis result, i.e., the orbitals on the Al cations do not affect in the optical processes. (ii) The sum of the birefringences and the SHG coefficients of the respective $(BO_3)^{3-}$ and $(YO_6)^{9-}$ anionic groups is larger than the original values. This is due to the fact that the orbitals on the oxygen atoms linked with the neighbor anionic groups are used twice in the real-space atom-cutting procedures. (iii) The $(BO_3)^{3-}$ anionic groups contribute more than 90% to the anisotropy of refractive indices and about 40% to the overall SHG coefficient. Conversely, the contribution of the $(YO_6)^{9-}$ anionic group to the birefringence is very small, but its contribution to the SHG effect is much more pronounced than that of the $(BO_3)^{3-}$ anionic group. The detailed structural analysis (see Fig. 6) shows that the $(YO_6)^{9-}$ group is a heavily deformed octahedron; the angles formed by the vertex oxygen, central yttrium, and base oxygen inside vary from 71.2 to 119.4°, far from those (= 90°) in a regular octahedron. In addition, the symmetry of the (YO_6) octahedron belongs to the point group, *D*3, which would result in the small anisotropy of the first-order optical effects (birefringence) but the large microscopic second-order optical susceptibility (SHG). In fact, the NLO crystals containing deformed (MO_6) octahedra (M = transition metal) usually have very large SHG coefficients, as in the cases of $LiNbO_3$, $KNbO_3$, $BaTiO_3$, LiTaO3, etc.[19]

These analysis results are very different from those in the KBBF-type NLO crystals where the $(BO_3)^{3-}$ anionic groups almost determine the birefringence and SHG effects.[18] The (YO_6) octahedra, but not the $(BO_3)^{3-}$ anionic groups, make the dominant contributions to the large SHG effect in YAB. This explains the reason why YAB has a much larger SHG coefficient compared to the KBBF-type NLO crystals. In practice, a similar situation also occurs in other borate NLO crystals, such as BiB_3O_6, in which the extremely large SHG coefficients ($d_{eff} \sim 3.2$ pm/V) are mainly attributed to the $(BiO_4)^{5-}$ anionic groups, rather than the B-O groups.[20]

TABLE II. Comparison of the refractive index and SHG coefficents derived from the atom-cutting method and the original values.

	n_e	n_o	Δn	d_{11}(pm/v)
Al^{3+}	1.0483	1.0525	0.0042	−0.001
BO_3^{3-}	1.3666	1.4362	0.0696	0.685
YO_6^{9-}	1.4290	1.4385	0.0095	1.421
Original	1.7011	1.7698	0.0687	1.657

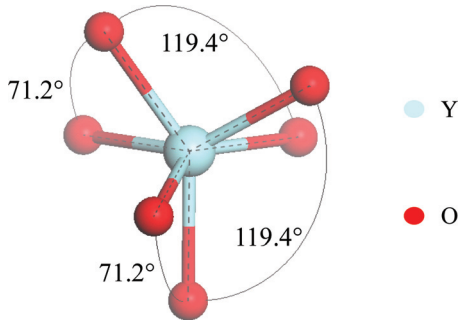

FIG. 6. (Color online) Geometry of the (YO_6) octahedron in YAB. Some angles formed by the vertex oxygen, central yttrium, and base oxygen are indicated.

IV. CONCLUSION

The first-principles electronic band structures calculation was carried out to study the optical properties of YAB. It is shown that the top of the valence bands are dominated by the O 2*p* orbitals, while the bottom of the conduction bands are mainly composed of Y 4*d* and B 2*p* orbitals. Based upon the electronic structure, the refractive indices and SHG coefficients were calculated, which are in good agreement with the experimental values. The combined SHG-weighted electron density analysis with the real-space atom-cutting method revealed that the $(BO_3)^{3-}$ anionic groups have a dominant contribution to the linear optical properties, while the (YO_6) octahedra play a virtual role to the SHG effects in YAB. We believe that understanding the mechanism for the optical response in YAB would enable us to find and design new UV NLO crystals in a more efficient manner.

ACKNOWLEDGMENTS

This work was supported by 973 project (Grant Nos. 2010CB630701, and 2011CB922204), the NSF of China (Grant No. 91022036) and the Special Foundation of the President of the Chinese Academy of Sciences. M.H.L. acknowledges NCHC and the NSC Grant No. NSC 97-2112-M-032-004-MY2 in Taiwan.

[1] A. A. Ballman, Am. Mineralogist **47**, 1380 (1962).
[2] A. A. Filimonov, N. I. Leonyuk, L. B. Meissner, T. I. Timchenko, and I. S. Rez, Krist. Tech. **9**, 63 (1974).
[3] D. Rytz, A. Gross, S. Vernay, and V. Wesemann, Proc. SPIE. **6998**, 14 (2008).
[4] X. Chen, H. Liu, and N. Ye, J. Synth. Cryst. **38**, 545 (2009) (in Chinese).
[5] Z. S. Lin, Z. Z. Wang, C. T. Chen, S. K. Chen, and M. H. Lee, Chem. Phys. Lett. **367**, 523 (2003).
[6] Z. S. Lin, Z. Z. Wang, C. T. Chen, S. K. Chen, and M. H. Lee, J. Appl. Phys. **93**, 9717 (2003).
[7] H. Huang, Z. S. Lin, L. Bai, Z. G. Hu, and C. T. Chen, J. Appl. Phys. **106**, 103107 (2009).
[8] C. T. Chen, B. C. Wu, A. D. Jiang, and G. M. You, Sci. Sin., Ser. B (Engl. Ed.) **28**, 235 (1985).

[9]J. Lin, M. H. Lee, Z. P. Liu, C. T. Chen, and C. J. Pickard, Phys. Rev. B **60**, 13380 (1999).
[10]Y. H. Wang, L. L. Wang, and H. D. Li, J. Appl. Phys. **102**, 013711 (2007).
[11]W. Kohn and L. J. Sham, Phys. Rev. **140**, A1113 (1965).
[12]J.E. Sipe and E. Ghahramani, Phys. Rev. B **48**, 11705 (1993).
[13]Z. S. Lin, J. Lin, Z. Z. Wang, and C. T. Chen, Phys. Rev. B **62**, 1757 (2000).
[14]M.-H. Lee, C-H. Yang, and J.-H. Jan, Phys. Rev. B **70**, 233104 (2004).
[15]M.-H. Lee, C.-H. Lo, and Z. S. Lin, et al. (unpublished).
[16]M. Cococcioni and S. de Gironcoli, Phys. Rev. B **71**, 035105 (2005).
[17]S. L. Dudarev, G. A. Botton, S. Y. Savrasov, C. J. Humphreys, and A. P. Sutton, Phys. Rev. B **57**, 1505 (1998).
[18]C. T. Chen, Z. S. Lin, and Z. Z. Wang, Appl. Phys. B **80**, 1 (2005).
[19]C. T. Chen, "Development of New NLO Crystals in the Borate Series", in Laser Science and Technology, an International Handbook, edited by V. S. Letokhov, C. V. Shank, Y. R. Shen, and H. Walther (Harwood, Chur, Switzerland 1993), Vol. **15**, Chap. 1.
[20]Z. S. Lin, Z. Z. Wang, C. T. Chen, and M. H. Lee, J. Appl. Phys. **90**, 5585 (2001).
[21]C. T. Chen, G. L. Wang, X. Y. Wang, and Z. Y. Xu, Appl. Phys. B **97**, 9 (2009).
[22]N. Ye, W. Zeng, B. C. Wu, and C. T. Chen, Z. Kristallogr. - New Cryst. Struct. **213**, 452 (1998).
[23]Z. G. Hu, T. Higashiyama, M. Yoshimura, Y. Mori, and T. Sasaki, Z. Kristallogr. **214**, 433 (1999).
[24]Z. G. Hu, M. Yoshimura, Y. Mori, and T. Sasaki, J. Cryst. Growth **260**, 287 (2004).
[25]V. V. Filippov, I. T. Bondar, N. V. Kuleshov, N. I. Leonyuk, V. V. Mal't-sev, and O. V. Pilipenko, J. Opt. Technol. **74**, 717 (2007).